

# 3D nanotube-based composites produced by laser irradiation

S.A. Ageeva, I.I. Bobrinetskii, V.I. Konov, V.K. Nevolin, V.M. Podgaetskii, O.V. Ponomareva, V.V. Savransky, S.V. Selishchev, M.M. Simunin

**Abstract.** 3D nanocomposites have been fabricated through self-assembly under near-IR cw laser irradiation, using four types of multiwalled and single-walled carbon nanotubes produced by chemical vapour deposition, disproportionation on Fe clusters and cathode sputtering in an inert gas. The composites were prepared by laser irradiation of aqueous solutions of bovine serum albumin until the solvent was evaporated off and a homogeneous black material was obtained: modified albumin reinforced with nanotubes. The consistency of the composites ranged from paste-like to glass-like. Atomic force microscopy was used to study the surface morphology of the nanomaterials. The nanocomposites had a 3D quasi-periodic structure formed by almost spherical or toroidal particles 200–500 nm in diameter and 30–40 nm in visible height. Their inner, quasi-periodic structure was occasionally seen through surface microfractures. The density and hardness of the nanocomposites exceed those of microcrystalline albumin powder by 20% and by a factor of 3–5, respectively.

**Keywords:** nanotubes, 3D composite, laser.

## 1. Introduction

One important issue in nanoengineering is the search for ways of designing three-dimensional (3D) macroscopic composites, which might open up the possibility of creating nanomaterials possessing unique properties. Typically, one has to deal with essentially planar 2D structures consisting of carbon nanotubes (CNTs) on orienting silicon substrates, which are used in a variety of electronic devices: field emission displays, molecular capacitors and others [1–3]. Exceptions include gels prepared by mixing CNTs with

ionic liquids [4, 5] and polymer- or titanium-matrix nanopaper containing CNTs [6, 7].

In the absence of any electric- or magnetic-field orienting effects, CNTs (especially single-walled carbon nanotubes, SWCNTs) form disordered agglomerates (tangles) kept together by relatively weak, van der Waals forces (binding energy of  $\sim 5 \text{ kJ mol}^{-1}$  [2]). Such agglomerates can be broken (untangled) by a variety of techniques [8, 9].

CNTs, in principle, appear the most suitable material for producing 3D nanocomposites through self-assembly provided CNT agglomerates can be reoriented. One of the missing coordinates of the nanotubular skeleton can be set by laser irradiation, whose influence in this case must, in particular, compete with the van der Waals forces.

Podgaetskii et al. [10] described a process for the fabrication of 3D nanocomposites via laser irradiation of aqueous dispersing solutions of proteins, bovine serum albumin (BSA) and human serum albumin (HSA), with small additions of CNTs. Water evaporation through radiative heating of the solutions led to the formation of a black CNT-reinforced material. The origin of the quasi-ordered state of the nanocomposites thus prepared has not yet been fully understood. Thus, the assumed orienting effect of laser irradiation on the degree of ordering in nanocomposites warrants further investigation.

The choice of albumin as a solution component was prompted by the initial ‘agglutination’ of the products and also by reports that albumin solutions had been successfully used in laser tissue welding [11–13]. In addition, albumin enables a considerable reduction in the separation of CNT solutions compared to aqueous nanotube solutions because of the increase in solution viscosity owing to the possible CNT functionalisation (attachment of functional groups) with albumin [2].

## 2. Materials and methods

We used several types of CNTs: multiwalled CNTs (MWCNTs) I [14] and II [15], produced by catalytic pyrolysis; SWCNTs III [16], prepared by the HipCO process; and SWCNTs IV [17], produced by the carbon arc method.

The key step in the preparation of MWCNTs I and II was thermocatalytic dissociation of a carbon-containing gas mixture on metallic catalysts (CVD process). MWCNTs I were produced on a nickel catalyst in a chamber with its inner part of a low thermal conductivity ceramic and its outer part of high-temperature steel. After pumping to a pressure  $P \sim 60 \text{ mbar}$ , the chamber was filled with ethanol

S.A. Ageeva State Scientific Centre for Laser Medicine, Studencheskaya ul. 40, 121165 Moscow, Russia; e-mail: geinic@yandex.ru;

I.I. Bobrinetskii, V.K. Nevolin, V.M. Podgaetskii, S.V. Selishchev,

M.M. Simunin Moscow State Institute of Electronic Technology (Technical University), proezd 4806 5, Zelenograd, 124498 Moscow, Russia; e-mail: podgaetsky@yandex.ru;

V.I. Konov, V.V. Savransky Natural Science Center, A.M. Prokhorov General Physics Institute, Russian Academy of Sciences, ul. Vavilova 38, 119991 Moscow, Russia; e-mail: vik@nsc.gpi.ru;

O.V. Ponomareva OOO NPF DELTARUS, Likhachevskii proezd 5b, Dolgoprudnyi, 141700 Moscow region, Russia; e-mail: ponomareva.05@mail.ru

Received 12 March 2008; revision received 27 November 2008

Kvantovaya Elektronika 39 (4) 337–341 (2009)

Translated by O.M. Tsarev

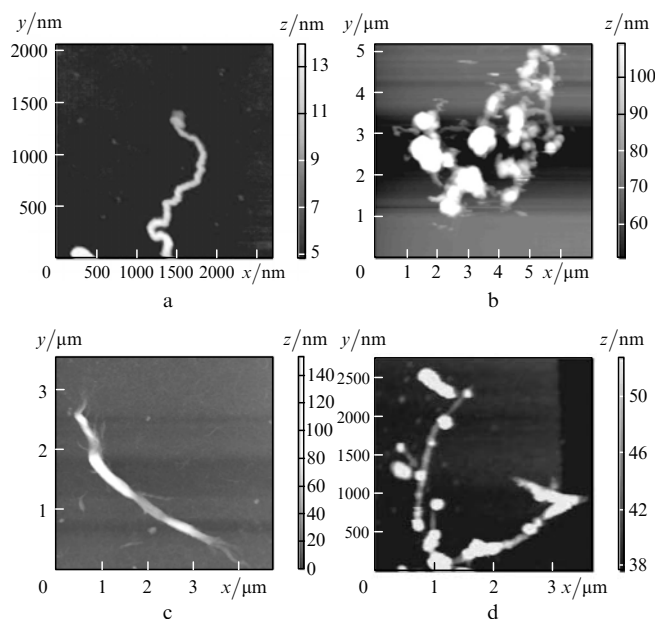


**Figure 1.** Topographic images obtained on a Solver P47 scanning probe microscope: (a) MWCNTs I, (b) MWCNTs II, (c) SWCNTs III and (d) SWCNTs IV.

vapour heated to  $\sim 600^\circ\text{C}$ . The nanotubes ranged in outer diameter  $D$  from 3 to 30 nm (Fig. 1a).

MWCNTs II (Taunit) were produced using a propane-butane mixture heated to  $600\text{--}680^\circ\text{C}$ . After acid treatment, the nanotubes ( $D = 20\text{--}40$  nm, average length  $L \leq 2$   $\mu\text{m}$ ) (Fig. 1b) were sufficiently pure. The material was easy to disperse, did not scatter and did not cake. It could be uniformly dispersed in organic and inorganic liquids in the presence of surfactants.

SWCNTs III were produced by disproportionation on Fe clusters prepared using an  $\text{Fe}(\text{CO})_5$  catalyst in flowing carbon dioxide, which was passed through a heated reactor at high pressure. The nanotubes (Fig. 1c) were fluorinated to remove the catalyst to an atomic fraction of Fe in the range 1%–3.5%. Their dimensions ( $L \sim 1$   $\mu\text{m}$ ,  $D = 0.7\text{--}1.4$  nm) could be tuned by varying the  $\text{CO}_2$  pressure.

The chamber for the preparation of SWCNTs IV (NanoCarbLab) was pumped down to  $\sim 10^{-4}$  Pa and then filled with an inert gas (argon or helium). Next, a discharge was initiated, which caused thermal sputtering of a graphite cathode. The anode contained small amounts of transition and rare-earth metals as catalysts. The weight fraction of SWCNTs (Fig. 1d) was  $\sim 80\%$ .

The structure of the CNTs and nanocomposites was examined on Solver P4 and Solver P47 scanning probe microscopes. Their laser optical systems measured the probe tip deflection, determined by the surface topography and physical properties of the specimen.

Figure 1 illustrates the surface structure of the CNTs. It can be seen that the MWCNT diameter considerably exceeds the SWCNT diameter (by several nanometres). The nanotubes range in length up to several microns (or even more). In Figs 1c and 1d, one can see inclusions (most likely, amorphous carbon particles) on the SWCNT surface.

The CNTs were added to an aqueous BSA solution (20%–25%) prepared by mixing in a magnetic stirrer and/or sonication for several hours slightly above room temperature.

The nanotube concentration in working solutions prepared in the same manner as the BSA solutions was  $1\text{--}3$   $\text{g L}^{-1}$ . The solutions were decanted (to remove the precipitate) and treated in the presence of a surfactant.

### 3. Results and discussion

The quality of the working solutions was verified by measuring their density, viscosity and absorption spectra (Figs 2, 3). In the UV to near-IR spectral region (400–1000 nm), the absorbance of the solutions decreases systematically with increasing wavelength (Fig. 2). With increasing temperature, the density of the solutions increases (Fig. 3a), whereas their kinematic viscosity decreases in a narrow temperature range and varies little above  $25^\circ\text{C}$  (Fig. 3b). When stored in a household refrigerator, the solutions retain their properties for several weeks.

The experimental arrangement for irradiation of solutions included a radiation source, a support with a collet chuck (for securing an optical fibre and thermocouple) and a stage with a beaker (sample support). It also included a digital remote thermocouple sensor (DT 832 multimeter)

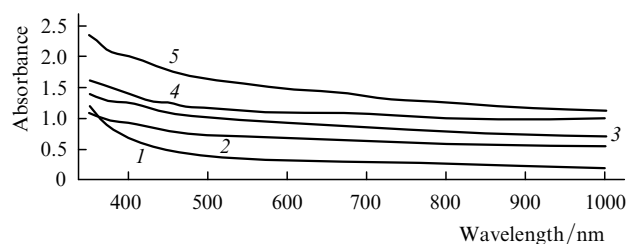


**Figure 2.** Absorption spectra of aqueous 25% BSA solutions containing (3) MWCNTs I, (5) MWCNTs II, (1) SWCNTs III and (2, 4) SWCNTs IV; (2) decanted solution. The thickness of the solution layer is 2 mm, and the nanotube concentration is (3) 1, (1, 2, 4) 2 and (5) 3  $\text{g L}^{-1}$ .

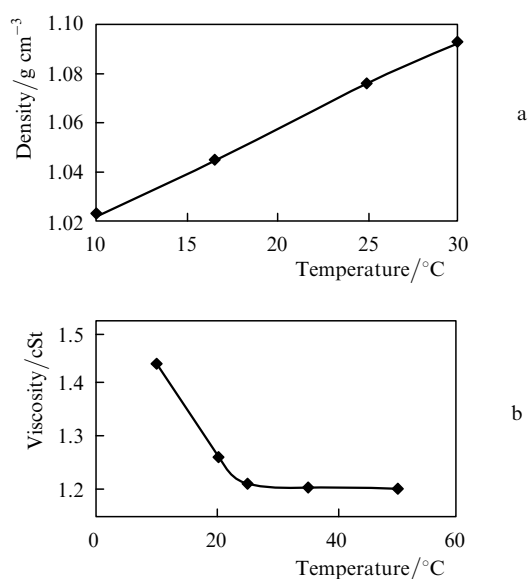


**Figure 3.** Temperature dependences of (a) density and (b) kinematic viscosity for an aqueous 25% BSA solution containing MWCNTs II. The thickness of the solution layer is 2 mm, and the nanotube concentration is 3  $\text{g L}^{-1}$ .

and an Optris MiniSight remote infrared thermometer. The radiation source was an LMP IRE-Polyus fibre-coupled cw diode laser ( $\lambda_g = 0.97 \mu\text{m}$ ,  $P \sim 10 \text{ W}$ ) fitted with a green laser aiming module ( $\lambda_g = 0.53 \mu\text{m}$ ) [18]. The solution was placed in a glass tube  $\sim 20 \text{ mm}$  in diameter (with no stirring).

The laser beam, with the spot diameter on the solution surface equal to the tube diameter, was directed downwards along the tube axis. Irradiation was continued until the liquid was evaporated off and a homogeneous black nanocomposite was obtained on the bottom of the tube. Whereas the denaturation temperature of pure BSA is  $60^\circ\text{C} - 70^\circ\text{C}$ , the nanocomposite was monolithic at considerably higher temperatures, up to  $\sim 200^\circ\text{C}$ .

The quality of the nanomaterial, assessed from its hardness, colour uniformity and the absence of whitish zones of denaturated albumin, depended on the incident intensity and irradiation time (see below). The consistency of the material ranged from rubber-like (at relatively low laser fluences) to glass-like. The weight of the product was 20% to 70% below that of the precursor solution.

The laser irradiation results are illustrated in Fig. 4, which shows topographic images of samples prepared by abrasively grinding the nanocomposites on a silicon substrate or by spreading (and drying) a droplet of wetted material between two plates.

The images were obtained by atomic force microscopy, by scanning an oscillating cantilever tip over the nanomaterial surface: light areas represent elevations, and dark areas represent depressions (towards the observer).

As seen in Figs 4a–4d, the nanomaterials based on MWCNT I and MWCNT II have a 3D quasi-periodic structure formed by almost spherical or toroidal particles 200–500 nm in diameter and 30–40 nm in visible height.

To remove bacterial material that might be present in the nanocomposites, they were UV-irradiated (PRK-4 lamp, 3 min,  $\sim 20\text{-cm}$  distance) and iodinated (3 min in an  $\sim 10\text{-ml}$  tube containing iodine crystals). The topographic images of the irradiated (Fig. 4c) and iodinated samples (MWCNTs I)

were similar to those of the as-prepared material (Fig. 4a), indicating that the samples were unlikely to be contaminated.

The SWCNT-based nanomaterials had a more complex surface morphology. In the case of SWCNTs III, the inner, quasi-periodic structure was seen through surface microfractures (Figs 4e–4g). In the case of SWCNTs IV (Fig. 4h), the structure was only partially periodic.

By analogy with previous results [10], it is reasonable to assume that the spheres (Figs 4a–4c) and similar particles (Figs 4e, 4h) seen in the structure of the nanomaterials are related to the presence of coiled nanotubes. The material between the nanotubes is albumin, reinforced with CNTs.

Prior to density ( $\rho$ ) measurements, 10–15 samples of each nanocomposite, 3–4 mm in size, were dried at room temperature. After determining their weight on an analytical balance, the samples were placed in a graduated cylinder half-filled with high-purity benzene (Nefras S 50/170), and their volume was determined.

The measured densities (90% confidence level) are listed in Table 1. It follows from these data that all our samples have nearly the same density, which exceeds that of microcrystalline albumin powder by 10%–20%.

The Vickers hardness  $H_V$  of the nanocomposites was determined with a PMT-3 microhardness tester: the material was indented with a diamond indenter in the form of a right pyramid with a square base. Polished specimens were mounted in grooves made in Textolite substrates and were fixed with Supermonolit epoxy. The substrates were

**Table 1.** Density and hardness of the nanocomposites.

Material	Density/ $\text{kg m}^{-3}$	Hardness/MPa
MWCNTs I	1220 $\pm$ 80	140–180
MWCNTs II	1200–1300	150–250
SWCNTs III	1250	130–200
SWCNTs IV	1200–1300	150 $\pm$ 20
BSA	1110	50–60
Poly(methyl methacrylate)	1160	200–300

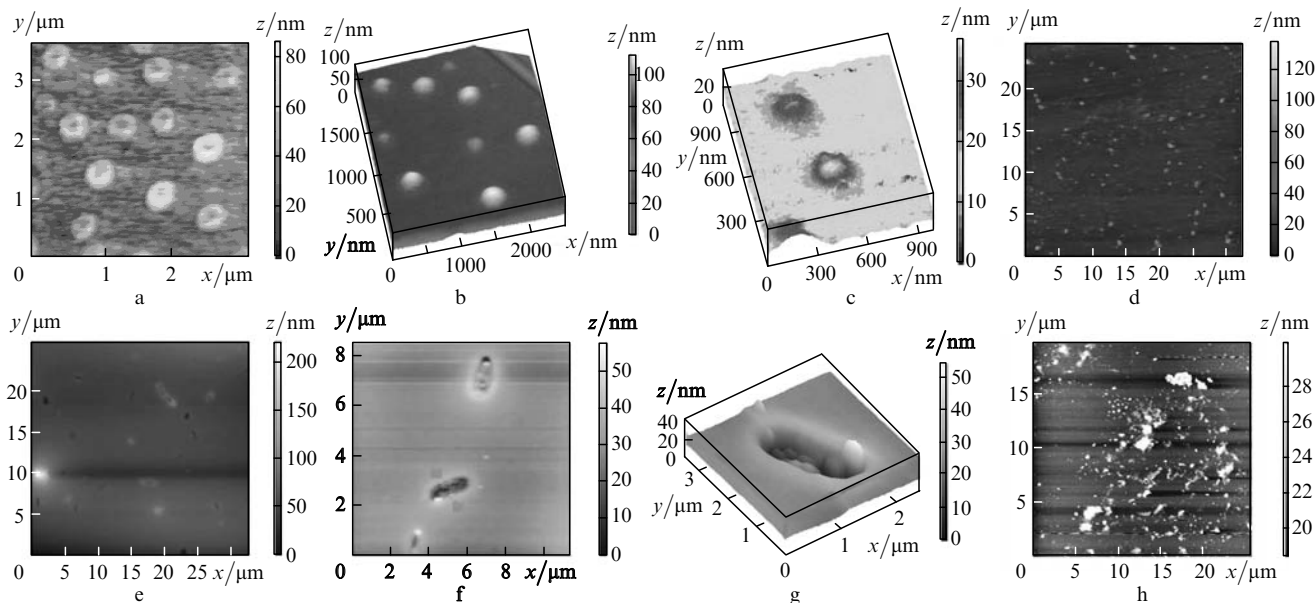


**Figure 4.** Topographic images of nanomaterials based on (a–c) MWCNTs I, (d) MWCNTs II, (e–g) SWCNTs III and (h) SWCNTs IV; (b, c) Solver P7 and (a, d–h) Solver P47 scanning probe microscopes; (b) after iodination, (c) after UV irradiation.

secured to the  $x - y$  table of the tester beneath the diamond indenter. The specimen surface was strictly parallel to the substrate backside. The indent diagonals were measured at indentation loads from 0.5 to 200 g.

The measured  $H_V$  values are listed in Table 1 (90% confidence level). The nanocomposites have  $H_V = 130 - 250$  MPa, which exceeds the microhardness of albumin by a factor of 3–5 and is comparable to that of poly(methyl methacrylate), a widely used polymeric material (organic glass). The observed scatter in  $H_V$  may be due to inhomogeneity of the nanocomposites. Moreover, their hardness depended on moisture content.

Microscopic examination showed that the nanomaterials contained micron-sized particles capable of distorting the expected inner structure of the nanotubular skeleton. The absorption spectra of the working solutions (Fig. 2) also attest to insufficient purity of the nanotubular material: there are no bands characteristic of CNTs with metallic or semiconducting properties. Therefore, the purity of the nanotubular component is crucial to the quality of the materials studied.

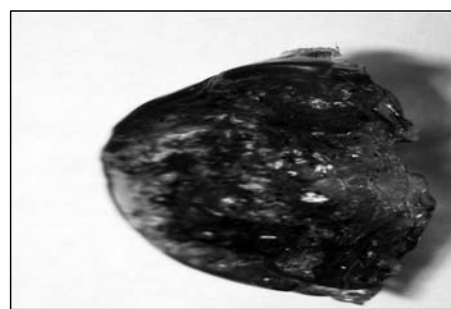
Note that alternative processes for the fabrication of nanocomposites from albumin solutions and CNTs (using thermal and ultrasonic methods) were unsuccessful: the albumin decomposed to form flakes, without combining with nanotubes. 3D composites can also be produced by sonicating aqueous BSA solutions containing CNTs (for  $\sim 10$  h at  $\sim 0.5$ -kW power) or by thermostating such solutions, but the resultant materials are brittle and have a layered, flaky structure, with little or no bonding between the albumin and nanotubes, as illustrated in Fig. 5. Also shown in Fig. 5 is the nanocomposite produced by laser irradiation of an aqueous BSA solution containing SWCNTs IV. The nanocomposites prepared from the four types of CNTs studied here can be stored at room temperature (or in a refrigerator) with no visible changes in their properties.

#### 4. Conclusions

3D nanocomposites with a nanotubular skeleton embedded in modified albumin were prepared by laser irradiation of aqueous albumin solutions containing carbon nanotubes. The nanocomposites have a quasi-ordered structure, which may be due to the orienting effect of laser radiation incident along the normal to the surface of the solution. The density of the nanocomposites exceeds that of microcrystalline albumin powder by 10%–20%, and their hardness exceeds the hardness of albumin by a factor of 3–5 and is comparable to that of poly(methyl methacrylate).

The described noncontact laser processing method for the fabrication of 3D quasi-periodic nanomaterials using aqueous protein solutions of nanotubes can be utilised to produce implant filler materials. The method is safe in that no pathological flora can persist in the nanocomposites and has the advantage of significant flexibility.

**Acknowledgements.** This work was supported in part by the RF Ministry of Education and Science (Project No. 02.513.11.3425) and the Russian Foundation for Basic Research (Grant No. 06-08-00624). The authors are grateful to E.D. Obraztsova for useful discussions and to M.A. Tavrizova for her assistance in the experimental work.



a



b



c

**Figure 5.** Nanocomposite prepared via laser irradiation (a) and pieces of composites prepared by sonication (b) and thermostating (c) using MWCNTs II.

#### References

- Harris P.J.F. *Carbon Nanotubes and Related Structures* (Cambridge: Cambridge Univ. Press, 1999).
- Rakov E.G. *Nanotrubki i fullereny* (Nanotubes and Fullerenes) (Moscow: Universitetskaya Kniga, Logos, 2006).
- Morinobu E., Takuya H., Yoong Ahn K., Hiroyuki M. *Jap. J. Appl. Phys.*, **45**, 4883 (2006).
- Fukushima T., Kosaka A., Ishumura Y., Yamamoto T., Takigava T., Ishii N., Aida T. *Science*, **300**, 2072 (2003).
- Bazhenov A.V., Fursova T.N., Kolesnikov N.N., Borisenko D.N., Timonina A.V., Turanov A.N., Baulin V.E., Dolganov P.V., Osip'yan Yu.A. *Izv. Akad. Nauk, Ser. Fiz.*, **71**, 684 (2007).
- Dong W., Cogbill A., Zhang T., Ghosh S., Tian Z.R. *J. Phys. Chem. B*, **110**, 16819 (2006).
- Sirivisoort S., Yao C., Xiao X., Sheldon B.W., Webster T.J. *Nanotechnology*, **18**, 365102 (2007).
- O'Connell M.J., Bachilo S.M., Huffman C.B., Moore V.C., Strano M.S., Haroz E.H., Rialon K.I., Boul P.J., Noon W.H., Ma C.K.J., Hauge R.H., Weisman R.B., Smalley R.E. *Science*, **297**, 593 (2002).
- Tausenev A.V., Obraztsova E.D., Lobach A.S., Chernov A.I., Konov V.I., Konyashchenko A.V., Kryukov P.G., Dianov E.M. *Kvantovaya Elektron.*, **37**, 205 (2007) [*Quantum Electron.*, **37**, 205 (2007)].

10. Podgaetskii V.M., Savransky V.V., Simonin M.M., Kononov M.A. *Kvantovaya Elektron.*, **37**, 801 (2007) [*Quantum Electron.*, **37**, 801 (2007)].
11. Nevorotin A.I. *Vvedenie v lazernuyu khirurgiyu* (Introduction to Laser Surgery) (St. Petersburg: Spetslit, 2000).
12. Simhon D., Halpern M., Brosh T., Vasilyev T., Ravid A., Tennenbaum T., Nero Z., Katzir A. *Annals Surgery*, **245**, 206 (2007).
13. Ageeva S.A., Podgaetskii V.M., Selishchev S.V., Titkova D.A., Tomilova L.G. *Med. Tekh.*, **2**, 20, 2007.
14. Bobrinetskii I.I., Nevolin V.K., Simunin M.M. *Khim. Tekhnol.*, **8**, 58 (2007).
15. Tkachev A.G., Mishchenko S.V., Artemov V.N., Negrov V.L., Blinov S.V., Turlakov D.A., Memetov N.R. *Nanotekhnika*, **2**, 17 (2006).
16. Shofner M.L., Khabashesku V.N., Barrera E.V. *Chem. Mater.*, **18**, 906 (2006).
17. [www.nanocarblab.com](http://www.nanocarblab.com).
18. Minaev V.P. *Kvantovaya Elektron.*, **35**, 976 (2005) [*Quantum Electron.*, **35**, 976 (2005)].